Research Square

Preprints are preliminary reports that have not undergone peer review.
They should not be considered conclusive, used to inform clinical practice,
or referenced by the media as validated information.

Integrating Rotary Drum Compost and Biomass-Derived 3D Anodes for Sustainable Bioelectricity Generation in Plant Microbial Fuel Cells

Kumar Sonu

kumar_sonuasg@yaoo.com

IIT Kanpur: Indian Institute of Technology Kanpur https://orcid.org/0000-0001-9166-1178

Manoj Kumar Tiwari

IITK: Indian Institute of Technology Kanpur

Research Article

Keywords: plant microbial fuel cell (PMFC), rotary-drum compost, bioelectricity generation, Portulaca grandiflora, biomass-derived anode, Cassia fistula

Posted Date: November 19th, 2026

DOI: https://doi.org/10.21203/rs.3.rs-11328968/v1

License: This work is licensed under a Creative Commons Attribution 4.0 International License.
Read Full License

Integrating Rotary Drum Compost and Biomass-Derived 3D Anodes for Sustainable Bioelectricity Generation in Plant Microbial Fuel Cells

Kumar Sonu [1*], *Manoj Kumar Tiwari* [1, 2, 3]

[1]*Kotak School of Sustainability, Indian Institute of Technology Kanpur, Kanpur 208016, India*

[2]*Department of Civil Engineering, Indian Institute of Technology Kanpur, Kanpur, 208016,*

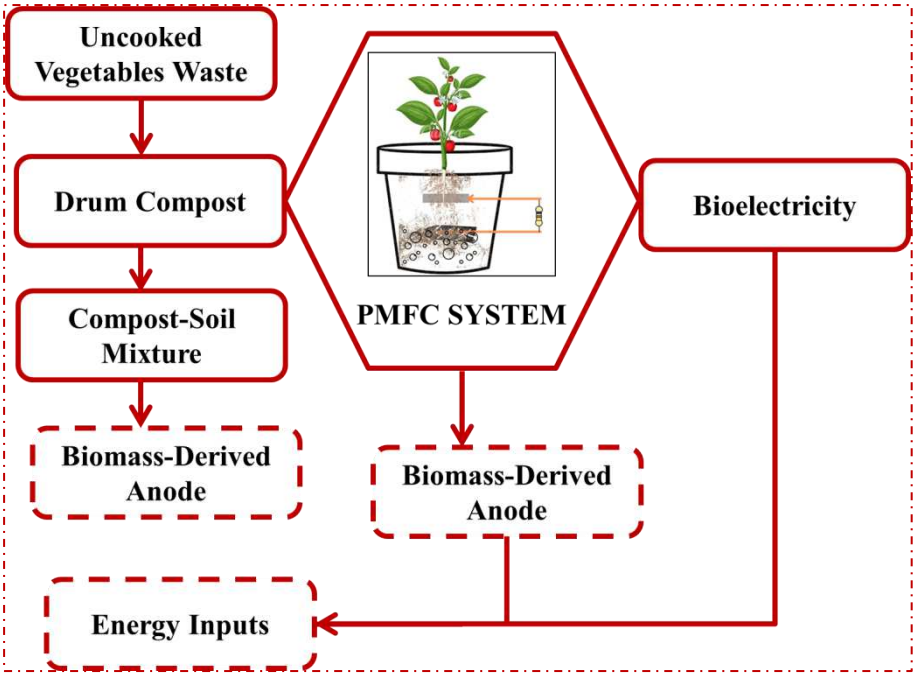
[3]*Centre for Environmental Science and Engineering, Indian Institute of Technology Kanpur, Kanpur 208016, India*

[*]*Corresponding author: Kumar_sonuasg@yahoo.com*

Highlights

- Moss rose (Portulaca grandiflora) was used as the plant species in the PMFC configuration.
- Maximum power density of 204 mW/m² was reported at a 50% compost-to-soil ratio.
- Microbial profiling showed the reported relative abundance of Geobacter, Shewanella, and Pseudomonas across compost treatments.
- Peak plant biomass yield (6.1 g/plant) was reported at 50% compost.
- EIS and CV were used to characterize the 50% compost treatment; these measurements were not performed comparatively across compost treatments.
- Preliminary direct materials cost was estimated at approximately INR 62 per unit; this estimate does not establish scalability or economic feasibility.
- The system combines vegetable-waste-derived compost and biomass-derived anode material within a PMFC configuration.

Graphical Abstract



Abstract

Plant microbial fuel cells (PMFCs) couple plant–microbe interactions in the rhizosphere with extracellular electron transfer to generate electricity while supporting plant growth. This study evaluated rotary-drum compost produced from uncooked vegetable waste as a soil amendment in PMFCs planted with Portulaca grandiflora and equipped with a three-dimensional carbonized Cassia fistula-pod anode. Compost fractions from 0 to 100% were investigated. The reported maximum power density was 204 mW m^{-2} at 50% compost, and the reported maximum dry plant biomass was 6.1 g $plant^{-1}$ at 50% compost. EIS and CV measurements were performed only for the 50% treatment; they characterize that treatment but do not independently establish the electrochemical mechanism behind the power-density result.

Keywords: plant microbial fuel cell (PMFC); rotary-drum compost; bioelectricity generation; Portulaca grandiflora; biomass-derived anode; Cassia fistula

1. Introduction

Microbial Fuel Cells (MFCs) have emerged as a promising bioelectrochemical technology for simultaneous wastewater treatment and renewable energy generation [1]. By harnessing the metabolic activity of electroactive microorganisms, MFCs convert chemical energy stored in organic matter into electricity through extracellular electron transfer (EET) processes at the anode [2]. Advances in system architecture, electrode materials, and microbial consortia have significantly enhanced the efficiency and output of MFCs over the past two decades [3].

Plant microbial fuel cells (PMFCs) use plant-derived rhizodeposits as substrates for microorganisms that transfer electrons to an anode. Their performance depends on interacting factors that include plant species, substrate chemistry and moisture, electrode configuration, microbial community, and operating conditions [7–17]. Compost amendment and electrode-material optimization have already been explored in microbial and plant microbial fuel cells; consequently, the novelty of a new PMFC configuration should not be based solely on combining a plant, compost, and a biomass-derived electrode. Instead, its contribution should be defined by the specific question tested, the quality of the comparative evidence, and the insight obtained from the results.

Despite prior advances, PMFC performance can remain limited by modest power output, variability in substrate properties, and uncertainty about the relationship between plant growth, microbial composition, and electron transfer [7–17]. Waste-derived compost may change nutrient availability, moisture retention, ionic conductivity, and microbial substrate supply simultaneously. These effects can improve plant growth without necessarily maximizing power output, because electrical performance also depends on electrode kinetics, mass transport, internal resistance, and the location and activity of electroactive microorganisms.

The present study examines a specific PMFC system comprising rotary-drum compost prepared from uncooked vegetable waste, Portulaca grandiflora, and a three-dimensional carbonized Cassia fistula-pod anode. The reported maximum power density (204 mW m^{-2}) and maximum dry biomass (6.1 g $plant^{-1}$) both occurred at 50% compost. These findings are specific to the tested configuration and operating conditions and should not be generalized beyond the experimental system.

Accordingly, the objectives were to: (i) screen compost-to-soil fractions for their association with PMFC electrical output; (ii) characterize the anode and its electrochemical response using the measurements collected; and (iii) compare plant-growth responses across compost fractions. The study does not establish that rotary-drum compost is generally superior to other composts, nor that the configuration is scalable; these questions require controlled head-to-head comparisons and longer-term evaluation.

The intended contribution is a treatment-level comparison of electrical performance and plant biomass in a PMFC using rotary-drum compost and a carbonized Cassia fistula-pod anode. The principal reported observation is that both the highest power density (204 mW m^{-2}) and highest dry biomass (6.1 g $plant^{-1}$) occurred at 50% compost. The results motivate further testing of compost amendment in this configuration but do not establish a universal optimum or general superiority over other PMFC systems.

This study aims to fill these gaps by:

- Evaluating different ratios of drum compost and soil on PMFC output.
- Investigating the bioelectrochemical performance of a 3D biomass-based anode.
- Monitoring the plant growth response (biomass and chlorophyll) under varying compost levels.

This study evaluates a specific integration of rotary-drum compost derived from uncooked vegetable waste with a biomass-derived three-dimensional anode in PMFCs. Compost amendment and electrode-material optimization have both been investigated in previous PMFC and MFC studies; therefore, the contribution here is the treatment-level assessment of compost fractions in this particular plant–compost–anode configuration. The reported 50% treatment showed the highest power density and plant biomass in the tested dataset.

2. Methodology

2.1 Drum Compost Preparation

Rotary-drum compost was prepared at IIT Kanpur from uncooked vegetable waste collected from campus hostels and canteens. The waste was shredded to below 10 mm and loaded into a 200-L horizontal drum. The drum was rotated manually three times per day; moisture was adjusted to approximately 55%, and mature compost was added at 5% (w/w) as inoculum. Composting continued for 21–25 days at ambient temperatures of 25–35 °C, followed by seven days of maturation. The compost was sieved to below 4 mm and stored before use. The reported final material was dark brown and granular, with pH 6.5–7.5 and approximately 12% organic carbon. Claims about pathogen status, heavy-metal compliance, or nutrient concentrations are limited to parameters supported by the corresponding analytical records.

2.2. Compost–Soil Mixture Preparation.

Compost was mixed with garden soil at tested fractions of 0%, 10%, 20%, 30%, 40%, 50%, 60%, 70%, 80%, 90%, and 100% by weight. Each unit received 3 kg of the mixture, which was homogenized and stabilized for 24 h before planting. Table 1 reports physicochemical properties for the control soil and the 50% compost-amended soil only; these values should not be generalized to every compost fraction. The contribution of individual parameters to power output was not isolated in this experiment.

Table 1. Physicochemical properties of control soil and soil amended with 50% drum compost.

Parameter	Control (0%)	50% Compost–Amended Soil
pH	7.2	6.5
Electrical Conductivity (dS/m)	0.45	0.95
Organic Carbon (%)	0.96	3.8
Total Nitrogen (%)	0.08	0.4
Available Phosphorus (mg/kg)	10.4	45.5
Available Potassium (mg/kg)	110	315
Moisture Content (%)	9.5	25.3
C/N Ratio	12	9.5
Bulk Density (g/cm^3)	1.42	1.12

2.3. Anode Preparation

Cassia fistula pods collected from the IIT Kanpur nursery were washed with distilled water, cut into approximately 50-mm pieces, and sun-dried for one week. The dried biomass was carbonized at a programmed heating rate of 10 °C min^{-1} to 550 °C. The available manuscript record does not unambiguously identify the furnace atmosphere or carbonization holding time; these details cannot be assigned from literature alone because air and inert-atmosphere carbonization produce materially different carbon products. They should be reported only after checking the laboratory record. After cooling, the carbonized material was wrapped in stainless-steel mesh to form a cylindrical anode approximately 8 cm long and 2 cm in diameter.

2.4. PMFC Setup and Operation

PMFCs were assembled in 5-L PVC pots containing the compost–soil medium. Each unit contained a three-dimensional carbonized Cassia fistula-pod anode and a carbon-fibre cathode and was planted with Portulaca grandiflora. PMFC literature emphasizes positioning the anode in the rhizosphere/root zone and placing the cathode in a more oxygenated region, while reporting electrode spacing because position and distance can affect proton transport, ohmic losses, and power output [6, 8]. The exact positions and spacing used in these experiments are not recoverable from the current manuscript record and are therefore not assigned an assumed numerical value here. Plant height and leaf chlorophyll were monitored weekly, and soil moisture was maintained at 60–70% of field capacity. No additional fertilizer was applied.

The plants received natural sunlight for approximately 10–12 h d^{-1} under semi-outdoor conditions. Reported daytime and nighttime temperatures were 25–32 °C and 18–22 °C, respectively. Pots were watered uniformly to maintain the target moisture range.

Cell voltage was monitored with a Haoyue DT830D digital multimeter twice daily. Polarization measurements were performed after the stabilization period using external resistors from 30 kΩ to 10 Ω. Current was calculated using I = V/R and power using P = VI; current density and power density were normalized to the reported anode area. The total operating duration, exact anode area used for normalization, resistor sequence, stabilization time at each resistance, and number of biological replicates must be taken from the original laboratory records; these values cannot be reconstructed reliably from published protocols. Results should be expressed as mean ± standard deviation where replicate-level data are available, and inferential statistics should be retained only where the underlying data support them. For EIS, published MFC protocols commonly use a small AC perturbation (often 5–10 mV) over a broad frequency range, with 100 kHz to 1 mHz being a commonly described range; these are literature benchmarks, not verified settings for the present experiment [34]. The CV reference/counter electrodes, electrolyte, scan rate, and potential window likewise need confirmation from the instrument files before being stated as actual settings.

2.5. Microbial Community Analysis

Microbial community analysis was described as 16S rRNA gene amplicon sequencing of rhizosphere and anode-associated samples. The reported workflow includes DNA extraction, amplification of the V3–V4 region, Illumina MiSeq sequencing, and QIIME 2/SILVA-based taxonomic assignment. The exact extraction kit, primer sequences, sequencing facility, software/database versions, sample numbers, biological replicates, quality-control thresholds, and accession number should be taken from the original sequencing report or facility records. These details cannot be reliably supplied from general literature without risking misreporting the experiment. Relative abundance is evidence of community composition, not a direct measurement of electrochemical activity or electron-transfer rate.

3. Results and discussion

3.1 Surface Morphology and Elemental Composition of Compost

The surface morphology of the compost sample was examined using Scanning Electron Microscopy (SEM), and the elemental composition was determined through Energy Dispersive X-ray Spectroscopy (EDX). As illustrated in Figure 1, the SEM micrograph reveals a highly heterogeneous and porous structure, characterized by numerous cavities and irregularly shaped aggregates. The porous architecture is indicative of advanced organic matter degradation, typically resulting from microbial activity during the composting process. These voids enhance the overall surface area, which is advantageous for microbial colonization, nutrient retention, and potential electrochemical applications in microbial fuel cells (MFCs).

The SEM image shows a heterogeneous surface with visible cavities and aggregates. The EDX spectrum shows the elements assigned in the original analysis. SEM appearance alone does not quantify specific surface area or prove that compost itself functions as a bioanode; in this study, compost is evaluated as a soil amendment/substrate in the PMFC.

The SEM/EDX results provide descriptive information about compost morphology and elemental composition. Interpretations concerning surface area, nutrient availability, and microbial colonization are limited to the measurements actually performed and are not inferred from surface appearance alone.

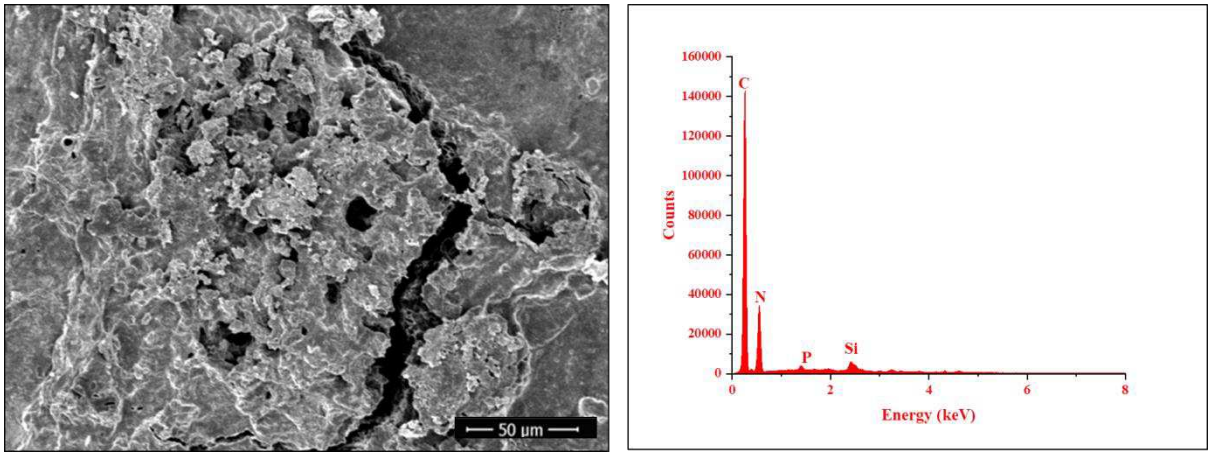


Figure 1 SEM image showing porous structure of compost and EDX spectrum

.

3.2. Electrochemical characterization of the 50% compost treatment

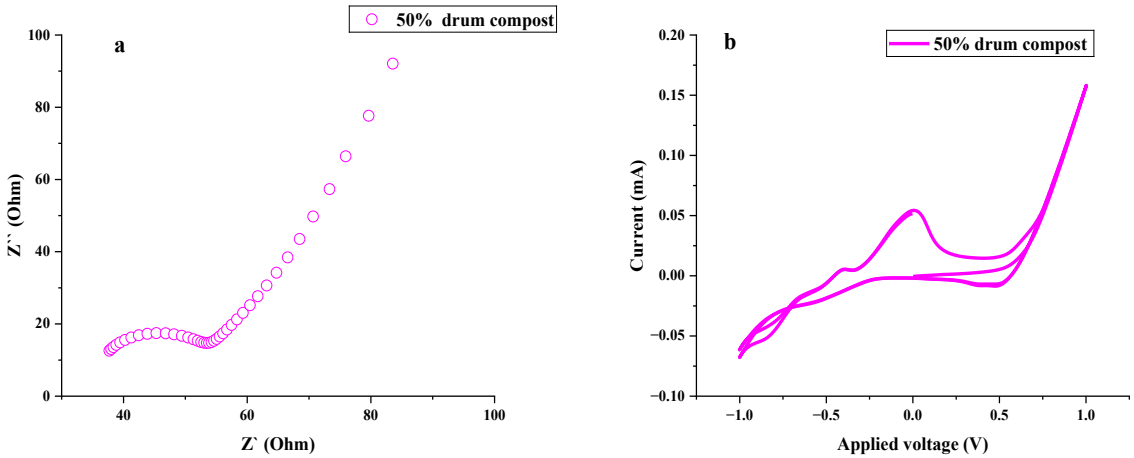


Figure 2. (a) EIS Nyquist plot for the 50% compost treatment. The ordinate is labelled −Z″ (Ω) where this matches the sign convention of the plotted impedance data. (b) CV response for the 50% compost treatment.

EIS and CV were performed for the 50% compost treatment only. In the Nyquist plot, the high-frequency intercept is commonly associated with solution/ohmic resistance, while the semicircle diameter can reflect charge-transfer resistance when supported by the data and an appropriate equivalent-circuit model. The low-frequency tail may include mass-transport effects; the linear diffusion-related region is generally associated with low rather than high frequencies. Numerical resistance values are not inferred from visual inspection alone. These data characterize the 50% treatment but do not provide a comparative test across compost fractions.

The CV trace for the 50% compost treatment shows the current response over the applied potential window. Its shape alone does not establish fully reversible redox behaviour or long-term reproducibility. Peak positions and current changes should be described in relation to the actual trace and scan rate. Because EIS and CV were performed only for the 50% treatment, they characterize that treatment but do not independently establish the mechanism behind the reported maximum power density. Comparative electrochemical measurements across compost fractions were not performed, so mechanistic conclusions remain limited.

3.3. FTIR and XRD of the anode before and after use

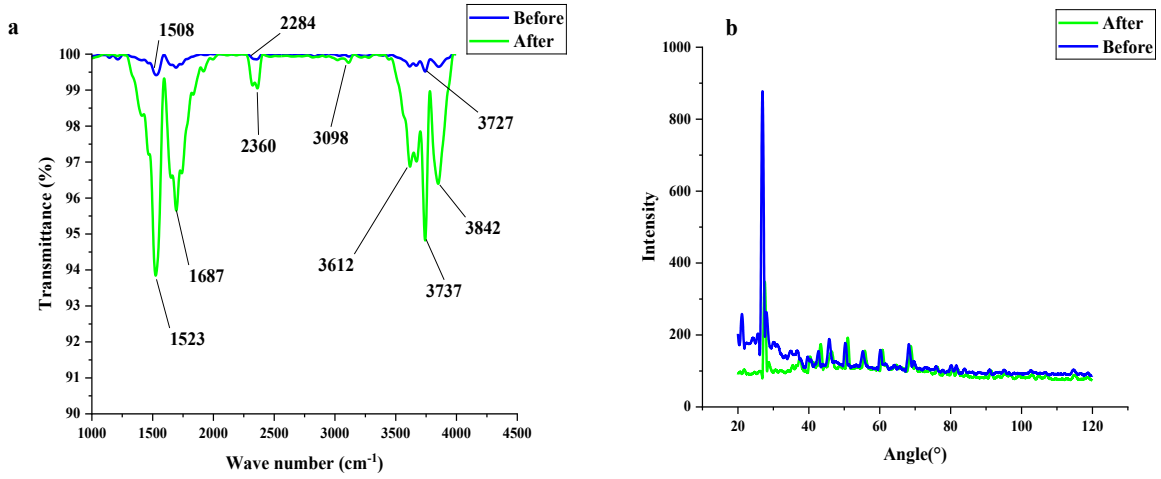


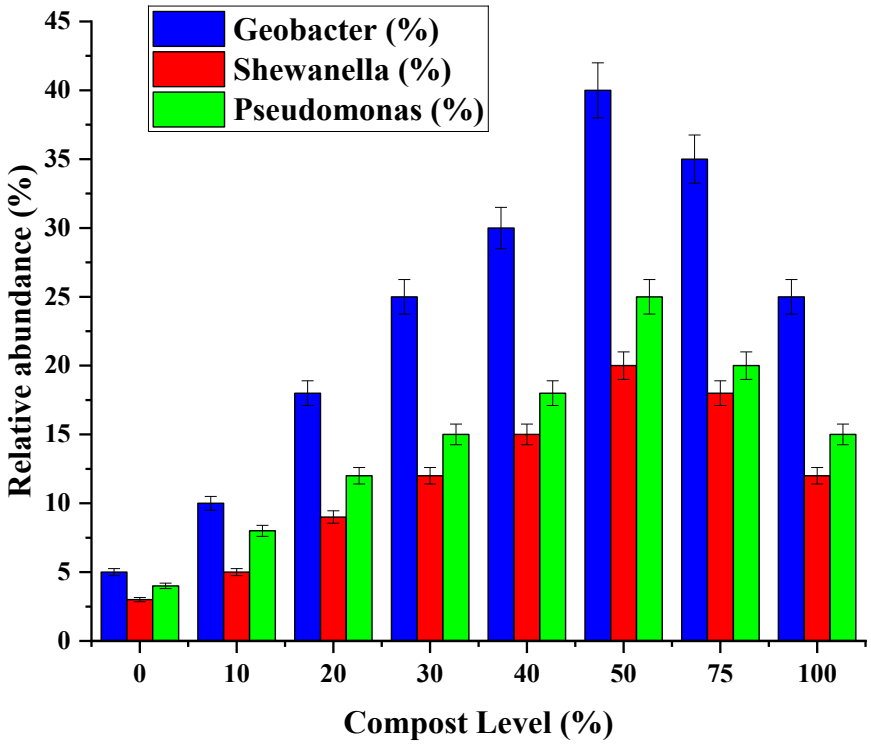
Figure 3 FTIR and XRD of the biomass-derived anode before and after PMFC operation

Figure 3a compares the FTIR spectra of the carbonized Cassia fistula-pod anode before and after PMFC operation. The annotated features in the displayed spectrum occur near 1508, 1523, 1687, 2284, 2360, 3098, 3612, 3727, 3737, and 3842 cm^{-1}. Peak assignments and the direction of intensity changes should be based on the displayed traces and the original spectral export. The spectra show changes between before- and after-use conditions; possible surface or biofilm-related effects should be presented as interpretations rather than proven mechanisms.

The XRD patterns compare the anode before and after PMFC operation. Interpretation is limited to the features visible in the displayed diffractograms. A feature near 26° 2θ may be consistent with carbonaceous ordering, but peak position and intensity alone do not establish changes in crystallite size or electrical conductivity; those claims require appropriate peak-width analysis and complementary measurements.

3.4. Microbial Community Structure in PMFC Substrates

Figure 4 presents the relative abundance of selected bacterial genera across compost treatments. The 50% treatment shows the highest plotted relative abundances for the listed genera and is also reported to have the maximum power density. Relative abundance describes the fraction of sequence reads assigned to a taxon, not its absolute cell number, metabolic state, electrode attachment, or electron-transfer activity. The data show an association between compost fraction and community composition but do not establish that any individual genus caused the observed power-density response.

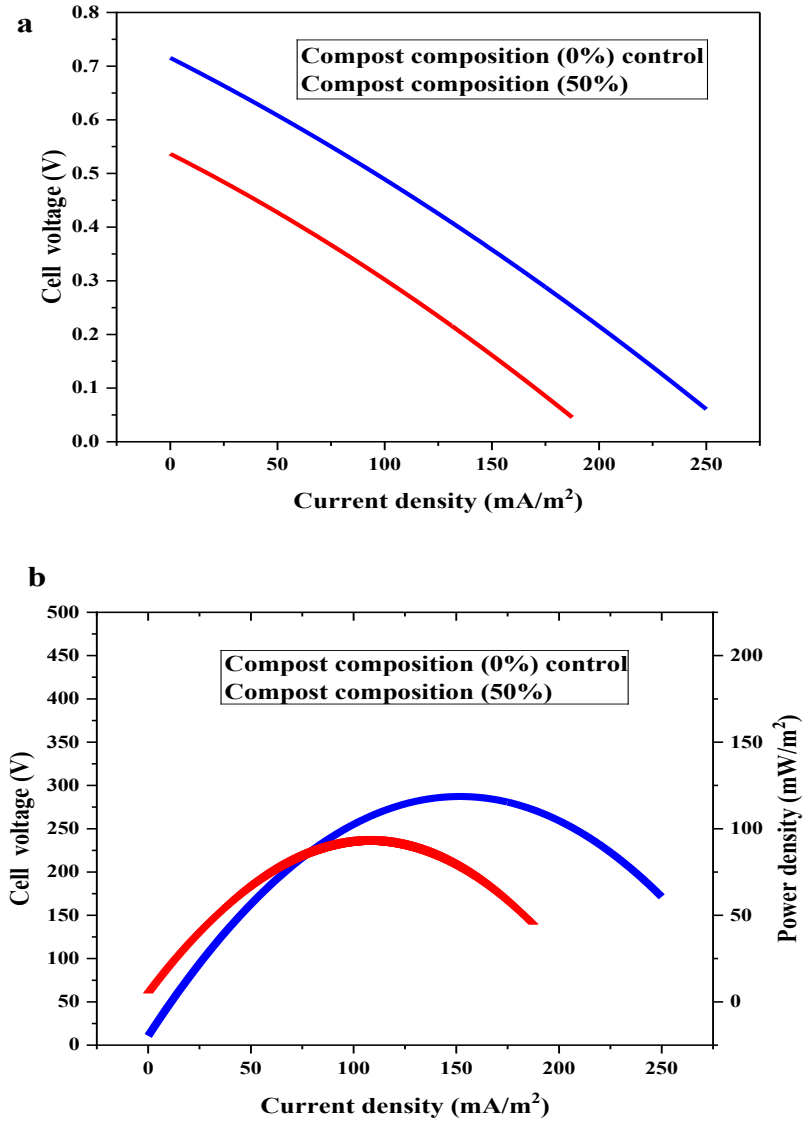


227

228 Figure 4. Relative abundance of selected bacterial genera across the compost fractions
229 represented in the figure. Error bars are shown as plotted.

230 **3.5. Polarization and Power Density Analysis**

231 Figure 5 compares polarization and power-density behaviour for the two treatments shown:
232 the 0% compost control and the 50% compost treatment. The 50% treatment is reported as
233 having the maximum power density of 204 mW m^{-2} in the broader treatment-screening
234 results. The figure presents polarization data for the 0% and 50% treatments only; it is not a
235 direct polarization comparison of every compost fraction. Mechanistic claims about internal
236 resistance or diffusion are not made without supporting measurements.



237

238 Figure 5. Polarization and power-density curves for the 0% compost control and 50%
239 compost treatment. Panel (a) presents cell voltage against current density. Panel (b) presents
240 the power-density relationship using the axes shown in the figure.

241 3.7. Dry Biomass Yield of Plant at Different Compost Compositions

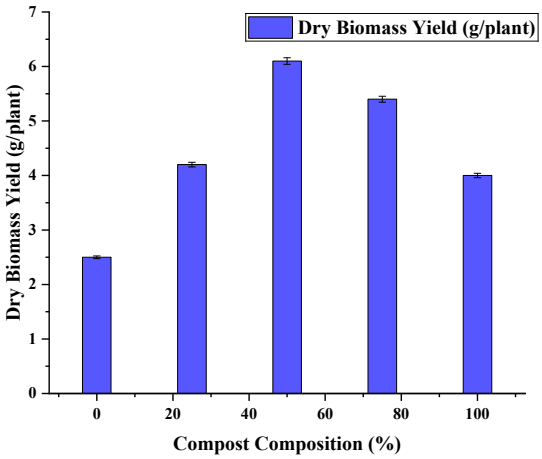


Figure 6. Dry plant biomass as a function of compost fraction, as plotted.

The reported dry biomass reached 6.1 g plant^{-1} at 50% compost, compared with 2.5 g plant^{-1} for the control. Plant biomass varied with compost fraction. Potential explanations for lower biomass at other fractions, including nutrient imbalance or salt accumulation, are hypotheses unless supported by corresponding measurements. Replicate number, variation, and statistical significance should be reported where available.

3.8 Comparison of Recent PMFC Studies Using Different Substrates and Electrodes

The reported maximum power density of 204 mW m^{-2} is comparable to values reported for other PMFC configurations, including approximately 200 and 220 mW m^{-2} for carbon-felt and graphite-based systems. It should not be described as a substantial power-output improvement over those systems. The contribution of the present configuration lies in evaluating locally available compost and a carbonized biomass-derived anode in a plant-based system. Cross-study comparisons should be interpreted cautiously because electrode area, reactor design, substrate, plant species, operating duration, and normalization methods may differ. The present results do not establish superiority, scalability, or lower life-cycle impact.

Table 2. Comparison of reported PMFC configurations and power densities (cross-study values should be interpreted cautiously because test conditions and normalization methods may differ).

Anode Material	Substrate Type	Max Power Density (mW/m^2)	Durability	Reference
Carbon felt + compost	Organic sludge	280	Moderate performance using commercial carbon felt	[20]
Graphene oxide-coated soil	Plant-MFC soil system	260	Requires advanced synthesis	[25]
Palm kernel shell carbon	Domestic wastewater	185	Bio-waste material, lower output	[34]
Tubular carbon electrodes	Wetland soil	220	Custom structure, high material prep cost	[33]
Epipremnum aureum root-based bioanode	Aquatic plant-PMFC	210	Plant-based system, good sustainability	[28]
Activated carbon + conductive polymer coating	Glucose solution	275	Requires chemical modification	[25]

Sugarcane bagasse carbon	Sugarcane wastewater	190	Similar biomass approach	[35]
3D *Cassia Fistula*-derived carbon	Drum compost (50%) + Soil	204	High performance with sustainable, low-cost anode material	This study

4. **Cost Analysis and Life Cycle Perspective**

The following estimate is a preliminary materials-only cost for one laboratory PMFC unit. It is not a full techno-economic assessment because labour, energy for drying and carbonization, instrumentation, maintenance, replacement, plant establishment, compost processing, and end-of-life costs may not be included. The environmental discussion is qualitative and is not a formal life-cycle assessment (LCA).

4.1. Cost Analysis

The listed components give an estimated direct materials cost of approximately INR 62 per unit under the assumptions in Table 3. This figure is not the total cost of ownership and does not establish economic feasibility at scale. Comparisons with other systems require comparable cost boundaries, capacity, electrode area, service life, and included components. Carbonization energy and labour are not quantified in the present estimate and should be identified as excluded where applicable.

The anode was prepared from carbonized Cassia fistula pods, while Portulaca grandiflora was the plant species. The INR 62 estimate is a preliminary direct-materials cost and is not evidence that deployment in rural or peri-urban settings is already feasible.

4.2. Energy Output and Economic Implications

At the reported maximum power density of 204 mW m^{-2} and an anode area of 0.01 m^2, the corresponding instantaneous power would be 2.04 mW if the stated area and normalization are correct. Cumulative energy cannot be inferred from peak power alone; any reported energy total must be calculated from time-resolved power data over the stated operating period and the calculation method should be provided.

The present cost estimate does not include a complete life-cycle cost or a comparison of levelized electricity cost. Accordingly, the system should not be described as economically feasible on the basis of materials cost alone. The potential value of compost diversion and plant growth is qualitative in this study and was not monetized.

4.3. Life Cycle Perspective

This section provides a qualitative discussion of resource use only. No formal life-cycle inventory, impact assessment, or comparative LCA was conducted; the points below are considerations for future assessment, not quantified environmental benefits.

- The system uses vegetable-waste-derived compost and locally available biomass. This supports a resource-circularity rationale, but the net environmental effect depends on the alternative waste-management route and the energy and materials consumed in composting, carbonization, and operation.
- The energy required for compost preparation, drying, carbonization, and operation was not quantified. Accordingly, low energy demand or energy payback cannot be claimed from the present data.

- Diversion of biodegradable waste may avoid some impacts associated with alternative disposal routes, but avoided methane emissions were not measured or modelled in this study. No quantified greenhouse-gas reduction is claimed.
- The reuse or recovery of the PVC pot, stainless-steel mesh, cathode, and compost–soil mixture would need to be assessed against local handling requirements. Safe reintegration of spent material was not established in this study.

A formal LCA, including a defined functional unit, system boundary, life-cycle inventory, allocation assumptions, and impact-assessment method, was not performed. The present discussion therefore cannot establish global-warming potential, energy payback, land-use impacts, or overall environmental superiority. A future assessment could use a recognized method after the required inventory data have been collected.

Table 3. Preliminary direct materials-cost estimate for one PMFC unit.

Component	**Description**	**Cost (INR)**
Drum Compost (50%)	Produced from uncooked vegetable waste	5.00
Garden Soil	Locally sourced, pre-existing	0.00
Cassia Fistula Bioanode	Carbonized biomass, mesh-wrapped	7.00
Stainless Steel Mesh	Anode reinforcement	10.00
Carbon Fiber Cathode	Commercially sourced	25.00
PVC Pot, Wiring, Misc.	Container and electrical hardware	15.00
Total per Unit		**62.00**

The cost estimate is an initial materials estimate only. Further experimental, engineering, and life-cycle work is needed before economic feasibility, environmental superiority, or scalability can be concluded.

Conclusion

This study evaluated PMFCs containing rotary-drum compost derived from uncooked vegetable waste, Portulaca grandiflora plants, and a three-dimensional carbonized Cassia fistula-pod anode. The reported screening results identified 50% compost as the treatment with the highest power density (204 mW m^{-2}) and the highest dry plant biomass (6.1 g $plant^{-1}$). EIS/CV measurements were performed only for the 50% treatment and do not independently establish the mechanism behind the power-density maximum. The displayed polarization figure compares the 0% and 50% treatments only. The study provides a system-specific initial assessment, not proof that the configuration outperforms existing PMFCs or is ready for scale-up. Further work should include comparative electrochemical measurements, fully documented electrode geometry and operating conditions, replicated microbial analyses, longer-term operation, and a formal techno-economic and life-cycle assessment.

Declarations

Ethics Declaration

Ethics declaration: Not applicable. This study did not involve human participants, human data, human tissue, or live vertebrate animals requiring ethical approval.

Ethics, Consent to Participate, and Consent to Publish

Ethics, Consent to Participate, and Consent to Publish declarations: Not applicable.

Funding

This research received no specific grant from any funding agency in the public, commercial, or not-for-profit sectors.

Competing Interests

The authors declare that they have no known competing financial interests or personal relationships that could have appeared to influence the work reported in this paper.

Data Availability Statement

The data supporting the findings of this study are available from the corresponding author upon reasonable request.

Author Contributions

Kumar Sonu: Conceptualization, methodology, investigation, data curation, formal analysis, visualization, and writing—original draft preparation. Manoj Kumar Tiwari: Supervision, project administration, and writing—review and editing.

References

1. Sonu, K., Syed, Z., & Sogani, M. (2019). Microbial fuel cell in domestic wastewater treatment plant–an innovative step towards energy generation and waste reduction.
2. Ma, J., Wang, L., Zhang, Y., & Jia, J. (2024). Fabrication of a Molybdenum Dioxide/Multi-Walled Carbon Nanotubes Nanocomposite as an Anodic Modification Material for High-Performance Microbial Fuel Cells. *Molecules*, *29*(11), 2541.

3. Ayanda, O. S., Mmuoegbulam, A. O., Okezie, O., Durumin Iya, N. I., Mohammed, S. A. E., James, P. H., ... & Badamasi, H. (2024). Recent progress in carbon-based nanomaterials: critical review. *Journal of Nanoparticle Research*, *26*(5), 106.
4. Abbas, S. Z., Beddu, S., Kamal, N. L. M., Rafatullah, M., & Mohamad, D. (2024). A review on recent advancements in wearable microbial fuel cells. *Journal of Environmental Chemical Engineering*, 112977.
5. Cheng, P., Zhang, Y., Li, M., Ma, H., Xu, W., Tan, X., ... & Jiang, L. (2024). Carbonaceous Anodes and Compatible Exoelectrogens in High-Performance Microbial Fuel Cells: A Review. *ACS ES&T Engineering*, *4*(3), 488-505.
6. Lepikash, R., Lavrova, D., Stom, D., Meshalkin, V., Ponamoreva, O., & Alferov, S. (2024). State of the art and environmental aspects of plant microbial fuel cells' application. Energies, 17(3), 752.
7. Kacmaz, G. K., & Eczacioglu, N. (2024). The mechanism of bioelectricity generation from organic wastes: Soil/plant microbial fuel cells. Environmental Technology Reviews, 13(1), 75-94.
8. Maddalwar, S., Nayak, K. K., Kumar, M., & Singh, L. (2021). Plant microbial fuel cell: Opportunities, challenges, and prospects. Bioresource Technology, 341, 125772
9. Sonu, K., Sogani, M., Syed, Z., Rajvanshi, J., & Pandey, S. C. (2024). Performance evaluation of Epipremnum aureum plant-based microbial fuel cell using composite anode made up of carbonized corncob and carbon rod. *Biomass Conversion and Biorefinery*, *14*(4), 5149-5156.
10. Kumar, S., Shinde, A., & Ghangrekar, M. M. (2024). Coal-based material as 3-D electrodes in continuous up-flow constructed wetland-microbial fuel cells. Sustainable Energy Technologies and Assessments, 69, 103913.

11. Sonu, K., Sogani, M., Syed, Z., Maheshwari, K., Rajvanshi, J., & Sengupta, N. (2024). Performance Investigation of Aloe Vera Plant-Based Microbial Fuel Cell Using Anode Constructed of Carbonized *Ipomoea Carnea*. *Waste and Biomass Valorization*, *15*(12), 7111-7121.
12. Chong, P. L., Chuah, J. H., Chow, C. O., & Ng, P. K. (2025). Plant microbial fuel cells: A comprehensive review of influential factors, innovative configurations, diverse applications, persistent challenges, and promising prospects. International Journal of Green Energy, 22(3), 599-648.
13. Meraj, A., & Jawaid, M. (2024). Plant biomass-based materials: an overview. *Plant Biomass Applications*, 1-24.
14. Martinez, R. D. R. (2024). Plant–microbial fuel cell for electrical generation through living plants: an internal resistance insight into the plant species used. *Clean Energy*, *8*(5), 45-53.
15. Ancona, V., Cavone, C., Grenni, P., Gagliardi, G., Cosentini, C., Borello, D., & Caracciolo, A. B. (2024). Plant microbial fuel cells for recovering contaminated environments. International Journal of Hydrogen Energy, 72, 1116-1126.
16. Chen, B., Li, L., Cai, W., & Garg, A. (2024). Bioelectricity generation in plant microbial fuel cells: Influence of vegetation density and unsaturated soil properties. *Biomass and Bioenergy*, *181*, 107053.
17. Sonu, K., Sogani, M., & Sharma, M. K. (2023). Performance evaluation of plant microbial fuel cell with Epipremnum aureum plant using composite anode made of corn cob and carbon rod. *International Journal of Environmental Studies*, *80*(1), 8-19.
18. Faruque, M. O., Rudra, S., Rahman, M. K. R., Hossen, I., Hossain, M. A., Mustakim, M., ... & Uddin, S. B. (2024). Floristic composition and biodiversity patterns in the

surroundings of Karanphuli river areas of Bangladesh. *Egyptian Journal of Botany*, *64*(3), 148-167.

19. Sharma, M., Jalalah, M., Alsareii, S. A., Harraz, F. A., Xue, W., Thakur, N., ... & Li, X. (2024). Microalgal cycling in the cathode of microbial fuel cells (MFCs) induced oxygen reduction reaction (ORR) and electricity: A biocatalytic process for clean energy. *Chemical Engineering Journal*, *479*, 147431.
20. Sharma, M., Jalalah, M., Alsareii, S. A., Harraz, F. A., Almadiy, A. A., Thakur, N., ... & Li, X. (2023). Fat, oil, and grease as new feedstock towards bioelectrogenesis in microbial fuel cells: Microbial diversity, metabolic pathways, and key enzymes. *Journal of Energy Chemistry*, *85*, 418-429.
21. Sharma, M., Jalalah, M., Alsareii, S. A., Harraz, F. A., Almadiy, A. A., Thakur, N., ... & Li, X. (2023). Fat, oil, and grease as new feedstock towards bioelectrogenesis in microbial fuel cells: Microbial diversity, metabolic pathways, and key enzymes. *Journal of Energy Chemistry*, *85*, 418-429.
22. ASTM, D., 2008. Standard test method for ash in the analysis sample of coal and coke from coal. (West Conshohocken: ASTM International).
23. Chaturvedi, K., Singhwane, A., Dhangar, M., Mili, M., Gorhae, N., Naik, A., ... & Verma, S. (2024). Bamboo for producing charcoal and biochar for versatile applications. *Biomass Conversion and Biorefinery*, *14*(14), 15159-15185.
24. Varshini, M., Ravichandran, K., Praseetha, P. K., Ayyanar, M., Ramalingam, S. J., Viji, A., & Manimekalai, R. (2024). Effective composite partnering of green synthesized rGO with SnO2: Ce: An eco-friendly approach using Cassia Fistula fruit pulp for photocatalytic and biomedical applications. *Ceramics International*, *50*(9), 14253-14267.

25. Sogani, M., Sonu, K., Syed, Z., & Rajvanshi, J. (2023, March). Preparation of biofertilizer blend from banana peels along with its application in agriculture and plant microbial fuel cell. In *IOP Conference Series: Earth and Environmental Science* (Vol. 1151, No. 1, p. 012034). IOP Publishing

26. Khedr, T. M., El-Sheikh, S. M., Kowalska, E., & Abdeldayem, H. M. (2021). The synergistic effect of anatase and brookite for photocatalytic generation of hydrogen and diclofenac degradation. *Journal of Environmental Chemical Engineering*, *9*(6), 106566.

27. Khedr, T. M., El-Sheikh, S. M., Kowalska, E., & Abdeldayem, H. M. (2021). The synergistic effect of anatase and brookite for photocatalytic generation of hydrogen and diclofenac degradation. *Journal of Environmental Chemical Engineering*, *9*(6), 106566.

28. Dhillon, S. K., & Kundu, P. P. (2022). Development of polypyrrole nanotube coated with chitosan and nickel oxide as a biocompatible anode to enhance the power generation in microbial fuel cell. *Journal of Power Sources*, *539*, 231595.

29. Yaqoob, A. A., Ibrahim, M. N. M., & Umar, K. (2021). Biomass-derived composite anode electrode: Synthesis, characterizations, and application in microbial fuel cells (MFCs). *Journal of Environmental Chemical Engineering*, *9*(5), 106111.

30. COMPOSTING, B. R. I. (2005). Control of heat generation during composting. *BioCycle*, *46*(1), 28.

31. Chen, L., Yang, M., Chen, Z., Xie, Z., Huang, L., Osman, A. I., ... & Yap, P. S. (2024). Conversion of waste into sustainable construction materials: A review of recent developments and prospects. *Materials Today Sustainability*, 100930.

32. Jahan, S., Ujjaman, S., Rahman, S., Sarker, B. C., Hossain, Z., & Kamal, M. (2022). Physicochemical properties and nutrient contents of compost as influenced by organic wastes and methods of composting. *Journal of the Indian Society of Soil Science*, *70*(1), 106-112.

33. Idris,, N. F., Gogoi, B., Saikia, R., Yousaf, B., Narayan, M., & Sarma, H. (2024). Encouraging circular economy and sustainable environmental practices by addressing waste management and biomass energy production. *Regional Sustainability*, *5*(4), 100174.

34. Idris, M. O., Yaqoob, A. A., Ibrahim, M. N. M., Noh, N. A. M., & Daud, N. N. M. (2022). Electrochemical measurements of microbial fuel cells (MFCs). In *Microbial Fuel Cells for Environmental Remediation* (pp. 41-64). Singapore: Springer Nature Singapore.

35. Idris, M. O., Guerrero-Barajas, C., Kim, H. C., Yaqoob, A. A., & Ibrahim, M. N. M. (2023). Scalability of biomass-derived graphene derivative materials as viable anode electrode for a commercialized microbial fuel cell: a systematic review. Chinese Journal of Chemical Engineering, 55, 277-292.

466

467